Journal of Institute of Science and Technology, 31(1), 231-238 (2026)
ISSN: 2467-9062 (print), e-ISSN: 2467-9240
https://doi.org/10.3126/jist.v31i1.84720

Research Article

CO-AXIAL CYLINDRICAL MODEL FOR TURBULENT AIRFLOW AND LAMINAR MUCUS FLOW IN CONSTRICTED HUMAN LUNG AIRWAYS

Janta Raut[1*], Vijai Shanker Verma[2]

[1]*Department of Mathematics, Thakur Ram Multiple Campus, Tribhuvan University, Birgunj, Nepal*
[2]*Department of Mathematics and Statistics, DDU Gorakhpur University, Gorakhpur, India*
[*]*Correspondence: janta19raut@gmail.com*

(***Received:*** *May 11, 2026;* ***Revised:*** *May 27, 2026;* ***Accepted:*** *June 9, 2026)*

ABSTRACT

In this paper, a two-layer cylindrical quasi-steady co-axial flow model is proposed to study the flow of air and mucus in the constricted human lung airways with a constant thickness of constriction influenced by a time-varying pressure gradient due to mild cough. Mucus exhibits Newtonian behavior in many pathological cases and therefore, in this paper mucus and air both are considered as incompressible Newtonian fluids. Mucus is supposed to be thicker and more viscous than air. The central core is assumed to have a quasi-steady turbulent flow of air while the surrounding mucus layer has a quasi-steady laminar flow of mucus. The model also incorporates the effect of the porosity parameter due to immotile cilia, which form a porous matrix. The study states that the flow rates of air and mucus decrease as mucus viscosity and constriction thickness increase. The study also states that the flow rates of air and mucus increase as the porosity parameter and pressure drop increase. The results obtained in this study compared with the results of various investigators working in related fields are found to be in good agreement.

Keywords: Constricted airways, Immotile cilia, Porosity parameter, Quasi-steady co-axial flow, Time varying pressure gradient

Mathematics Subject Classification: 76A05, 76Z05, 92B05, 92C10, 96Z05

INTRODUCTION

The human respiratory system has multiple defense mechanisms to keep us healthy. During inhalation, air travels in a branching structure as soon as it enters through the mouth or nose. At these bends, larger particles hit the sides of the airways, while smaller particles travel with the air. Large dust particles are captured by nasal hairs and deposited as sticky mucus, commonly referred to as phlegm. Sneezing, spitting, coughing, or swallowing are some of the ways that this mucus is periodically evacuated from the body as it slowly advances toward the outside. The mucus membranes of the bronchi and windpipe produce the mucus itself. Small projections that resemble hairs called cilia constantly push mucus in the direction of the mouth. The majority of the trapped particles are carried up the windpipe by the cilia, which move in coordinated waves. The mucus is either ingested or spit out once it gets to the mouth. Removing contaminants from the inspired air, such as aerosols, bacteria, viruses and carcinogens from tobacco smoke, is one of this mucus layer's main functions.

Respiratory diseases such as cystic fibrosis, chronic bronchitis, bronchial asthma, pneumonia, lung cancer, primary ciliary dyskinesia and many other respiratory diseases may result from ciliary failure, which reduces the ability to remove particles effectively and produces excess mucus, which can be evacuated through coughing or forced expiration. Coughing is the primary defense mechanism for clearing mucus in human beings with immotile cilia syndrome.

Several mathematical approaches and models have been studied in this area. King et al. (1993) proposed a planar two-layer fluid model for muco-ciliary clearance in lung airways. The model shows that mucus transport increases as shear stress and pressure drop increase. They have shown that the maximum rate of mucus transport occurs at a certain thickness of serous fluid. Kumar (2023) has investigated mucus transport in diseased airways by taking the influence of constriction in the airways and shown that the mucus flow rate reduces as the airway diameter increases. By considering the porosity parameter, pressure gradient, and shear stress caused by air motion, Raut et al. (2023) introduced a two-layer planar unsteady-state model.

The model shows that mucus flow rises as porosity, pressure gradient, air motion, and shear stress rise.

We aim to investigate a two-layer cylindrical co-axial flow in air and mucus regions in the constantly constricted airways. In this model, we assume that the air flow in the central core lumen is of quasi-steady and turbulent type whereas mucus flow surrounding the core lumen is assumed as quasi-steady state and laminar. We took into account the impact of the porosity parameter caused by the immotile cilia, which form a porous matrix in contact with epithelial walls.

MATERIALS AND METHODS

Mathematical model

In the real world, human lungs have cylindrical airways. Therefore, the flow of air and mucus in a lung airway is represented by a co-axial cylindrical tube geometry with a ciliated inner surface wall as shown in Figure 1. The core lumen is thought to be filled with air and encircled by a thick layer of mucus, which is then covered by a watery serous layer that has a much lower viscosity than the mucus. Due to an immediate pressure gradient during a slight cough, it is hypothesized that the air in the central core flows under quasi-steady-state turbulent circumstances, but the surrounding mucus flows under quasi-steady-state laminar conditions. The model also takes into account the influence of porosity induced by immotile cilia in the serous layer that forms a porous matrix with the epithelial wall. During mild cough, Reynolds number exceeds 4000 and flow becomes turbulent. We consider the mucus layer as constricted and tightened due to smooth muscles connected to the wall in the proposed model. This model is often applied in the context of muco-obstructive lung diseases such as cystic fibrosis, bronchitis, primary ciliary dyskinesia, severe asthma etc., where mucus is chronically overproduced.

The radius of the cylindrical tube varies with the constriction geometry and therefore, there exists following relation which gives the impact of constriction in the diseased state of the human lungs:

$$\mathrm{R_m} = \mathrm{R} - \delta \tag{1}$$

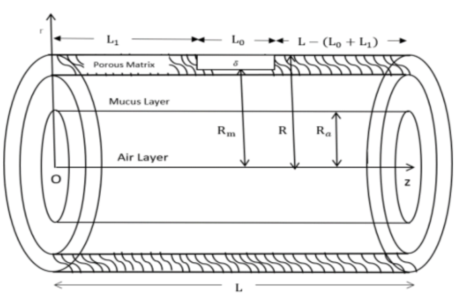

Figure. 1. Co-axial cylindrical tube geometry with constricted airways

here R denotes the radius of cylindrical tube, $\mathrm{R_m}$ denotes the radius of cylindrical tube in constricted area, $\delta(\ll \mathrm{R_m})$ is the thickness of constriction which is constant. We shall use Prandtl mixing length theory for quasi-steady equations in turbulent layers in cylindrical coordinates (Schlichting, 1960). The governing equations for the air and mucus flows under the above mentioned states in a cylindrical tube geometry as in the human lung airways can be written as:

Region I: Quasi Steady Turbulent Air Flow Region ($\mathbf{0 \leq r \leq R_a}$):

$$\frac{\partial p}{\partial z} = \frac{1}{r}\frac{\partial}{\partial r}(r\tau_a) \tag{2}$$

$$\tau_a = -\rho_a\, l_a^2 \tag{3}$$

Region II: Quasi Steady Laminar Mucus Flow Region ($\mathbf{R_a \leq r \leq R_m}$):

$$\frac{\partial p}{\partial z} = \frac{1}{r}\frac{\partial}{\partial r}(r\tau_m) \tag{4}$$

$$\tau_m = \mu_m \frac{\partial u_m}{\partial r} \tag{5}$$

where

z = axial coordinate along the cylindrical tube axis in the direction of flow,

r = radial coordinate perpendicular to the direction of fluid flow,

R_a = distance from the central axis to the mucus-air interface,

p = pressure across the layers,
τ_a = shear stress across air,
τ_m = shear stress across mucus,
ρ_a = density of air,
u_a = velocity component of the air in z-direction
u_m = velocity component of mucus in z-direction,
μ_a = viscosity of air, and
μ_m = viscosity of mucus.

By using Prandtl mixing length theory, l_a is assumed to be

$$l_a = l_0(R - r) \tag{6}$$

where l_0 is constant and is determined experimentally (Schlichting, 1960).

The governing equations can be solved by considering the following boundary and matching conditions:

Boundary Conditions:

$$\frac{\partial u_a}{\partial r} = 0, \qquad r = 0 \tag{7}$$

$$u_m = -\beta \tau_m, \quad r = R_m \tag{8}$$

Matching Conditions:

$$u_a = u_m, \qquad r = R_a \tag{9}$$

$$\tau_a = \tau_m, \qquad r = R_a \tag{10}$$

The negative sign in equation (8) is considered due to the negative value of τ_m in the mucus layer. Here, it is important to emphasize that β is the porosity parameter induced due to immotile cilia, which are saturated with the watery serous layer, forming a porous matrix with the epithelial walls in the airways. Equations (9) and (10) ensure that velocity and stresses are continuous at the mucus-air interface (Singh et al., 2021). The instantaneous pressure gradient created in the lung airways during coughing (mild cough) varies over time. Therefore, we may take

$$-\frac{\partial p}{\partial z} = P = P_0 f(t) \tag{11}$$

where t is the time and P_0 is a constant influenced by the intensity of the mild cough. As the cough duration increases, the intensity of mild coughing increases.

The function $f(t)$ for mild cough is assumed to follow the following relation:

$$f(t) = \begin{cases} \dfrac{3t^2}{8T_m}\left(1 - \dfrac{2t}{3T_m}\right), & 0 \le t \le T_m \\ \dfrac{9t}{32}\left(1 - \dfrac{9t}{10T}\right)^2, & T_m \le t \le \dfrac{T}{\alpha} \\ 0, & \dfrac{T}{\alpha} \le t \end{cases} \tag{12}$$

where $\alpha = 0.9$ and $T_m = 0.011$, T_m is the time when $f(t)$ is maximum and T is the cough duration.

To simplify the analysis, we can assume that the cough duration T spans from 0.030 seconds to 0.032 seconds. The graphical representation of $f(t)$ for mild cough given by equation (12) is shown in Figure 2.

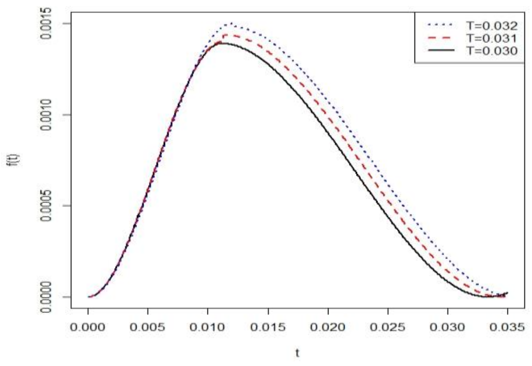

Figure 2. Graphical representation of $f(t)$ for different values of T

Analytical solution

Solving equations (2) - (5) by using boundary and matching conditions (6) - (10), the stress and velocity components in air and mucus layers are computed and are given as follows:

$$\tau_a = -\frac{Pr}{2} \tag{13}$$

$$\tau_m = -\frac{Pr}{2} \tag{14}$$

$$u_a = \frac{P}{4\mu_m}\left[R_m^2 + 2\beta\mu_m R_m - R_a^2\right] + \sqrt{\frac{PR}{2\rho_a l_0^2}}\left[\log\left|\frac{\sqrt{R}+\sqrt{R_a}}{\sqrt{R}-\sqrt{R_a}}\right| - \log\left|\frac{\sqrt{R}+\sqrt{r}}{\sqrt{R}-\sqrt{r}}\right| + \frac{2(\sqrt{r}-\sqrt{R_a})}{\sqrt{R}}\right] \tag{15}$$

$$u_m = \frac{P}{4\mu_m}\left[R_m^2 + 2\beta\mu_m R_m - r^2\right] \tag{16}$$

The volumetric flow rates in the air and mucus layers are respectively can be defined as follows:

$$Q_a = \int_0^{R_a} 2\pi r\, u_a dr \tag{17}$$

$$Q_m = \int_{R_a}^{R_m} 2\pi r\, u_m dr \tag{18}$$

Substituting the values of u_a and u_m in (17) and (18) respectively, we get

$$\frac{Q_a}{2\pi} = \frac{PR_a^2}{8\mu_m}(R_m^2 + 2\beta\mu_m R_m - R_a^2) + \sqrt{\frac{PR^5}{8\rho_a l_0^2}}\left[log\left|\frac{\sqrt{R}+\sqrt{R_a}}{\sqrt{R}-\sqrt{R_a}}\right| - 2\sqrt{\frac{R_a}{R}}\left(1 + \frac{R_a}{3R} + \frac{R_a^2}{5R^2}\right)\right] \quad (19)$$

$$\frac{Q_m}{2\pi} = \frac{P}{16\mu_m}(R_m^2 - R_a^2)(R_m^2 + 2K_1R_m - R_a^2) \quad (20)$$

The equation of continuity, which asserts that both Q_a and Q_m are constants, is used to determine the pressure decrease in each layer. Consequently, using equations (19) and (20), we obtain

$$-\frac{\partial p}{\partial z} = \frac{Q_a}{\pi}\left[\frac{8\mu_m}{R_a^2(R_m^2+K_1R_m-R_a^2)}\right] + \left[\frac{K_2K_3}{R_a^2(R_m^2+K_1R_m-R_a^2)}\right]^2 \quad (21)$$

$$-\frac{\partial p}{\partial z} = \frac{Q_m}{\pi}\left[\frac{8\mu_m}{(R_m^2-R_a^2)(R_m^2+2K_1R_m-R_a^2)}\right] \quad (22)$$

where $K_1 = 2\beta\mu_m$, $K_2 = \sqrt{\frac{R^5}{8\rho_a l_0^2}}\left[log\left|\frac{\sqrt{R}+\sqrt{R_a}}{\sqrt{R}-\sqrt{R_a}}\right| - 2\sqrt{\frac{R_a}{R}}\left(1 + \frac{R_a}{3R} + \frac{R_a^2}{5R^2}\right)\right]$ and $K_3 = \frac{1}{8\mu_m}$.

Replacing R_m by R for non-constricted regions, the pressure gradient for non-constricted regions $0 \le z \le L_1$ and $L_1 + L_0 \le z \le L$ become

$$-\frac{\partial p}{\partial z} = \frac{Q_a}{\pi}\left[\frac{8\mu_m}{R_a^2(R^2+K_1R-R_a^2)}\right] + \left[\frac{K_2K_3}{R_a^2(R_m^2+K_1R_m-R_a^2)}\right]^2 \quad (23)$$

$$-\frac{\partial p}{\partial z} = \frac{Q_m}{\pi}\left[\frac{8\mu_m}{(R_m^2-R_a^2)(R_m^2+2K_1R_m-R_a^2)}\right] \quad (24)$$

Define the pressure drop $\Delta P = p_0 - p_L$, where $p_0 = p$ at $z = 0$ and $p_L = p$ at $z = L$.

Now, using equations (21) and (23), we get

$$\Delta P = -\int_0^L dp = \int_0^{L_1}\left[\left\{\frac{K_2K_3}{R_a^2(R_m^2+K_1R_m-R_a^2)}\right\}^2 + \frac{Q_a}{\pi}\left\{\frac{8\mu_m}{R_a^2(R^2+K_1R-R_a^2)}\right\}\right]dz$$
$$+ \int_{L_1}^{L_1+L_0}\left[\left\{\frac{K_2K_3}{R_a^2(R_m^2+K_1R_m-R_a^2)}\right\}^2 + \frac{Q_a}{\pi}\left\{\frac{8\mu_m}{R_a^2(R^2+K_1R-R_a^2)}\right\}\right]dz$$
$$+ \int_{L_1+L_0}^{L}\left[\left\{\frac{K_2K_3}{R_a^2(R_m^2+K_1R_m-R_a^2)}\right\}^2 + \frac{Q_a}{\pi}\left\{\frac{8\mu_m}{R_a^2(R^2+K_1R-R_a^2)}\right\}\right]dz \quad (25)$$

Again, using the value of R_m from equation (1) in equation (25), we get

$$\Delta P = \frac{64\mu_m^2K_2^2(L-L_0)}{R_a^4(R^2+K_1R-R_a^2)^2}$$
$$+ \frac{64\mu_m^2K_2^2L_0}{R_a^4((R-\delta)^2+K_1(R-\delta)-R_a^2)^2} + \left(\frac{Q_a}{\pi}\right)\left[\frac{8\mu_m(L-L_0)}{R_a^2(R^2+K_1R-R_a^2)}\right] + \left(\frac{Q_a}{\pi}\right)\left[\frac{8\mu_mL_0}{R_a^2((R-\delta)^2+K_1(R-\delta)-R_a^2)}\right] \quad (26)$$

Now, let us suppose the following:

$$X = \frac{64\mu_m^2K_2^2(L-L_0)}{R_a^4(R^2+K_1R-R_a^2)^2} + \frac{64\mu_m^2K_2^2L_0}{R_a^4((R-\delta)^2+K_1(R-\delta)-R_a^2)^2} \quad (27)$$

$$Y = \frac{8\mu_m(L-L_0)}{R_a^2(R^2+K_1R-R_a^2)} + \frac{8\mu_mL_0}{R_a^2((R-\delta)^2+K_1(R-\delta)-R_a^2)} \quad (28)$$

Then, the equation (26) can be written as follows:

$$\Delta P = X + \frac{Q_a}{\pi}Y \quad (29)$$

from which the volumetric flow rate of air i.e. Q_a is found as follows:

$$Q_a = \frac{\pi}{Y}(\Delta P - X) \quad (30)$$

where X and Y are respectively given by equations (27) and (28).

Now, using equations (22) and (24), we get

$$\Delta P = -\int_0^L dp = \int_0^{L_1} \frac{Q_m dz}{\pi K_3 (R^2 - R_a^2)(R^2 + 2K_1 R - R_a^2)} + \int_{L_1}^{L_1+L_0} \frac{Q_m dz}{\pi K_3 (R_m^2 - R_a^2)(R_m^2 + 2K_1 R_m - R_a^2)}$$

$$+ \int_{L_1+L_0}^{L} \frac{Q_m dz}{\pi K_3 (R^2 - R_a^2)(R^2 + 2K_1 R - R_a^2)} \tag{31}$$

Again, using the value of R_m from equation (1) in equation (31), we get

$$\Delta P = \frac{Q_m}{\pi K_3}\left\{\frac{(L-L_0)}{(R^2-R_a^2)^2 + 2K_1 R (R^2 - R_a^2)} + \frac{L_0}{((R-\delta)^2 - R_a^2)^2 + 2K_1 (R-\delta)((R-\delta)^2 - R_a^2)}\right\} \tag{32}$$

from which the volumetric flow rate of mucus i.e. Q_m is found as follows:

$$Q_m = \pi K_3 \Delta P \left[\frac{(L-L_0)}{(R^2-R_a^2)^2 + 2K_1 R (R^2 - R_a^2)} + \frac{L_0}{((R-\delta)^2 - R_a^2)^2 + 2K_1 (R-\delta)((R-\delta)^2 - R_a^2)}\right]^{-1} \tag{33}$$

RESULTS AND DISCUSSION

To explore the impact of different model parameters on flow rates of air and mucus in trachea, the values of Q_a and Q_m given by equations (30) and (33) have been determined using the following standard values (Weibel, 1963; Shukla et al., 1999).

$R = 90.00 \times 10^{-2}\ cm, R_m = 38.45 \times 10^{-2}$ cm,

$R_a = 31.45 \times 10^{-2}$ cm, $t = 0 - 0.035$ sec,

$T = 0.035$ sec, $L = 1.0$ cm, $L_0 = 0.5$ cm,

$l_0 = 0.40$ cm, $P_0 = (1 - 10) \times 10^5$ gm cm^{-2} sec^{-2},

$\beta = 0 - 0.10$ gm cm^2 sec,

$\mu_m = 1.00 - 10.00$ poise, $\mu_a = 0.0002$ poise,

$\delta = 0 - 0.05$ cm, $\rho_a = 1.00 \times 10^{-3}\ gm\ cm^{-3}$

Various graphs using R software are plotted in figures (3 – 6) showing variations in flow rates Q_a and Q_m with time t

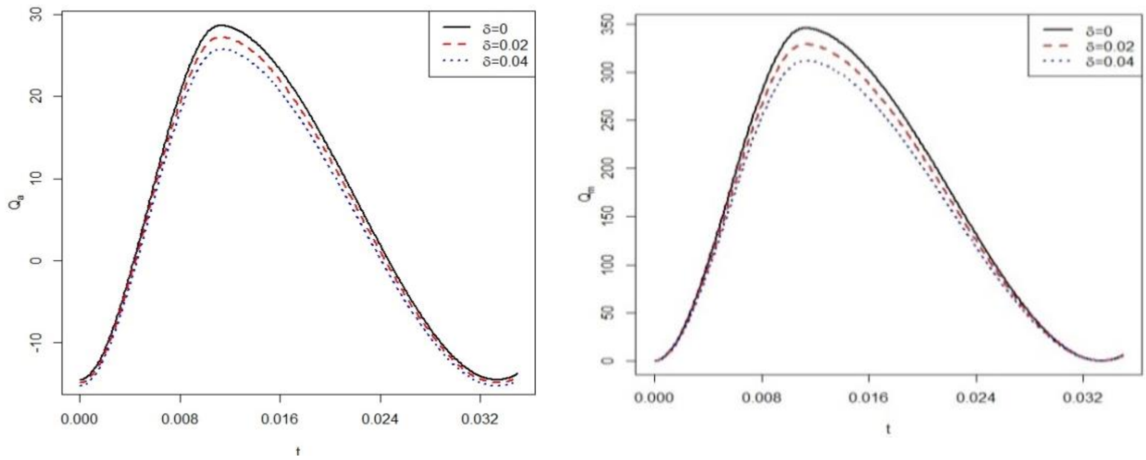

Figure. 3. Variations in Q_a and Q_m with t for distinct values of δ

Figure 3 illustrated the variations in flow rates of air and mucus with time t for distinct values of δ, while maintaining fixed values for T = 0.035 sec, $R = 90.00 \times 10^{-2}$cm, $R_m = 38.45 \times 10^{-2}$ cm, $R_a = 31.45 \times 10^{-2}$cm, L = 1.0 cm, L_0= 0.5 cm, $P_0 = 10 \times 10^5$ gm cm^{-2} sec^{-2} , β= 0.05 gm cm^{2}sec, $\rho_a = 1.00 \times 10^{-3} gm\, cm^{-3}$, μ_m = 1 poise and μ_a= 0.0002 poise. It is noted that as the constriction thickness δ increases, the flow rates of air and mucus both are giving a decreasing trend. These results are consistent with previous findings (Kumar et al., 2016).

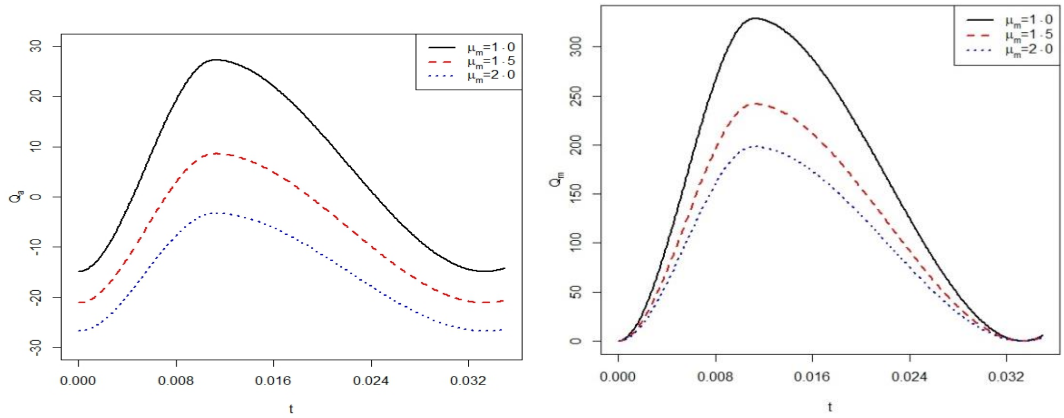

Figure. 4. Variations in $Q_a$and Q_m with t for distinct values of μm

Figure 4 depicts the variations in flow rates of air and mucus with time for distinct values of μ_m, while maintaining fixed values for $R = 90.00 \times 10^{-2}$cm, $R_m = 38.45 \times 10^{-2}$ cm, $R_a = 31.45 \times 10^{-2}$cm, T = 0.035 sec, L = 1.0 cm,L_0= 0.5 cm, $P_0 = 10 \times 10^5$ gm cm^{-2} sec^{-2} , β =0.05 gm cm^{2}sec, $\rho_a = 1.00 \times 10^{-3} gm\, cm^{-3}$, μ_a= 0.0002 poise and δ = 0.02 cm. The figure shows that air and mucus flow rates decrease as mucus viscosity μ_m increases. These results are consistent with previous findings (King et al., 1993; Verma & Tripathee, 2013; Verma & Rana, 2015; Kumar et al., 2016; Raut et al., 2023).

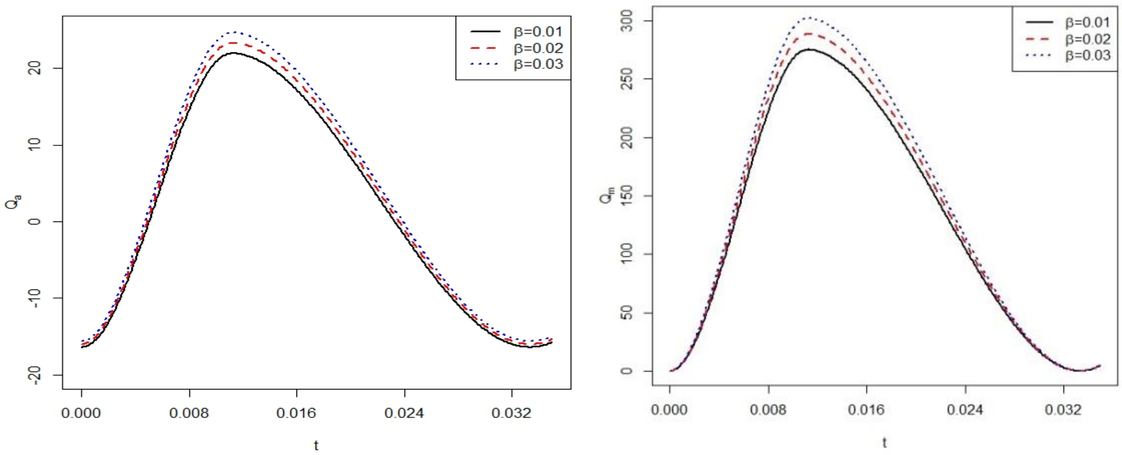

Figure. 5. Variations in Q_a and Q_m with t for distinct values of β

Figure 5 depicts the variations in flow rates of air and mucus with time t for different values of β, while maintaining fixed values for $R = 90.00 \times 10^{-2}$cm, $R_m = 38.45 \times 10^{-2}$ cm, $R_a = 31.45 \times 10^{-2}$cm, T = 0.035 sec, L = 1.0 cm, L_0= 0.5 cm, $\rho_a = 1.00 \times 10^{-3} gm\, cm^{-3}$, $P_0 = 10 \times 10^5$ gm cm^{-2} sec^{-2} , μ_m = 1 poise, μ_a= 0.0002 poise, δ = 0.02 cm (remove poise). The figure shows that air and mucus flow rates increase as the porosity parameter β increases. These results are consistent with previous findings (Sathpathi et al., 2003; Raut et al., 2023).

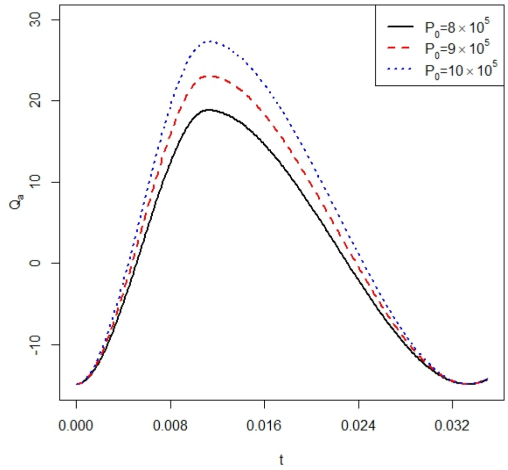

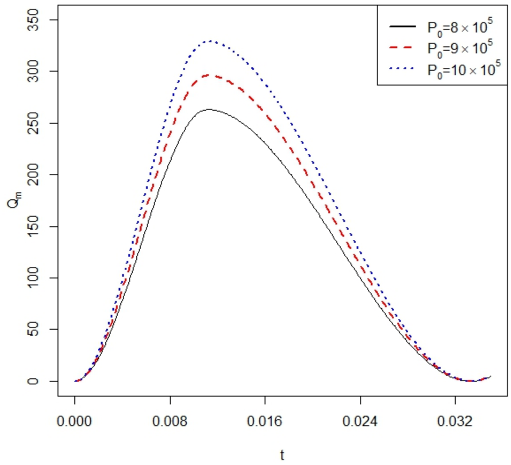

Figure 6. Variations in Q_a and Q_m with t for distinct values of P_0

Figure 6 depicts variations in flow rates of air and mucus with time for distinct values of P_0 and for fixed values of $R = 90.00 \times 10^{-2}$cm, $R_m = 38.45 \times 10^{-2}$ cm, $R_a = 31.45 \times 10^{-2}$cm, T = 0.035 sec, L = 1.0 cm, L_0= 0.5 cm, β= 0.05 gm cm^{2}sec, $\rho_a = 1.00 \times 10^{-3} gm\, cm^{-3}$, μ_m = 1 poise, μ_a= 0.0002 poise, δ = 0.02 cm. It is observed that the flow rates of air and mucus increase as the intensity of mild cough or the pressure drop in the two layers or gravitational acceleration increases. These results are consistent with previous findings (Agarwal et al., 1994; Verma & Tripathee, 2013; Verma & Rana, 2015).

CONCLUSION

A two-layer co-axial cylindrical model is presented in this study. It takes into account the stresses in air and mucus as well as the effect of mild cough which affects mucus flow and airflow in constricted airways. During mild cough, the Reynolds number exceeds 4000 and therefore, air is assumed to follow under quasi-steady turbulent flow regime, whereas the mucus is assumed to follow quasi-steady-state laminar flow. The model also incorporates the impacts of air-motion and the porosity parameter. The study shows that both mucus and air flow rates decrease with increasing constriction thickness. It has also been shown that mucus and air flow rates decrease with increase in mucus viscosity. Mucus and air flow rates are shown in increasing trend with increase in the porosity parameter. It has also be shown that mucus and air flow rates increase as the intensity of mild cough or the pressure gradient in the air and mucus layers increases. The proposed model validates the previous findings.

ACKNOWLEDGMENTS

The authors are grateful to the UGC, Nepal for providing financial support to this research.

AUTHORS CONTRIBUTION

Conceptualization: JR; Methodology: JR; Validation: VSV; Data Collection: JR; Data analysis: VSV; Writing original draft: JR; Review and Editing: VSV

FUNDING

None

ORCIDs

Janta Raut:
https://orcid.org/0009-0004-5850-5930
Vijai Shanker Verma:
https://orcid.org/0009-0009-4719-7908

CONFLICT OF INTEREST

The authors declare that there are no conflicts of interest regarding the publication of this article.

ETHICAL STATEMENT

The authors state that it is our original work and has not been previously published or submitted for publication elsewhere.

DATA AVAILABILITY STATEMENT

The data that supports the findings of this study are available from the corresponding author, upon reasonable request.

SUPPLEMENTARY INFORMATION

None

REFERENCES

Agarwal, M., King, M., & Shukla, J. B. (1994). Mucus gel transport in a simulated cough machine: Effects of longitudinal grooves representing spacings between arrays of cilia. *Biorheology, 31*, 11–19.

King, M., Agarwal, M., & Shukla, J. B. (1993). A planer model for muco-ciliary transport: Effect of mucus Visco-elasticity. *Biorheology*, *30*, 49–61.

Kumar, P. (2023). *Modelling and Analysis of mucus transport in diseased airways: effects of constriction of airway diameter*. Ph.D. Thesis, D. E. I. (Deemed University), Agra, India.

Kumar, P., Saxena, A., & Tyagi, A. P. (2016). Mathematical modelling of mucus transport in diseased airways with effects of constriction of airway diameter and mucus viscosity. *2016 3rd International Conference on Computing for Sustainable Global Development (INDIACom)*, 1832–1836.

Raut, J., Verma, V. S., & Rana, V. (2023). Mathematical Modelling Approach for Transport of Serous fluid and Mucus in Human Lung Airways. *Journal of Rajasthan Academy of Physical Sciences*, *22*(3–4), 257–270.

Satpathi, D. K., Kumar, B. V. R., & Chandra, P. (2003). Unsteady-state laminar flow of viscoelatic gel and air in a channel: Application to mucus transport in a cough machine simulating trachea. *Mathematical and Computer Modelling, 38*, 63–75.

Schlichting, H. (1960). *Boundary Layer Theory*. McGraw-Hill Book Company, Inc., New York.

Shukla, J. B., Chandra, P., Satpathi, D. K., & King, M. (1999). Some Mathematical model for mucus transport in lung due to forced expiration or cough. *Proc. International Conference on Frontiers of Biomechanics, Bangalore, India*.

Singh, Y., Shekhar, K., & Tyagi, A.P. (2021). Mathematical modelling of mucus transport in airways due to cough: quasi - steady state turbulent condition. *Series on Biomechanics, 35*(3), 69–84.

Verma, V. S., & Rana. V. (2015). Mucus transport in the human lungs: A mathematical Analysis. *Journal of Rajasthan Academy of Physical Sciences*, *14*(2)**,** 145–156.

Verma, V. S., Raut, J., & Rana, V. (2021). Role of Pressure Gradient and Porosity Parameter in Enhancing Mucus Transport in Lung Airways. *Journal National Academy of Mathematics*, *35*, 42–51.

Verma, V. S., & Tripathee, S. M. (2013). A planar model for muco-ciliary transport in the human tung: Effects of mucus visco-elasticity, cilia beating and porosity. *International Journal of Mathematical Modeling and Physical Sciences*, *1*(1), 19–25.

Weibel, E. R. (1963). *Morphometry of human lung*. Academic Press Inc., New York,